CLM - P 180

United Kingdom Atomic Energy Authority

RESEARCH GROUP

Preprint

AN ELECTROMAGNETICALLY ACTUATED FAST CLOSING SWITCH USING POLYTHENE AS THE MAIN DIELECTRIC

P. J. ROGERS
H. R. WHITTLE

Culham Laboratory
Abingdon Berkshire

1968

UNCLASSIFIED
(Approved for Publication)

CLM - P 180

AN ELECTROMAGNETICALLY ACTUATED FAST CLOSING SWITCH USING POLYTHENE AS THE MAIN DIELECTRIC

by

P.J. Rogers
H.R. Whittle

(Submitted for publication in Proceedings of the I.E.E.)

ABSTRACT

A switch consisting of two electrodes separated by a polythene sheet and which is closed by driving a rivet through the dielectric, so as to firmly join the electrodes, has operated in 40 kV circuits with peak currents up to 600 kA and passing a total charge of 2,500 coulombs.

The switch closes in about 50 μsec with shot to shot variations of ± 1 μsec. The metal-to-metal contact has a D.C. resistance of about 1 μΩ.

The rivet is driven by a hammer repelled from a fixed coil which is pulse energised from an auxiliary capacitor.

U.K.A.E.A. Research Group,
Culham Laboratory,
Abingdon,
Berks.

August, 1968 (SER)

C O N T E N T S

LIST OF SYMBOLS

B	Flux density in gap for resistive hammer.
B_o	Flux density in gap for perfectly conducting hammer.
B_c	Flux density on centre line of coil.
C	Driving circuit capacitor
C_v	Volumetric specific heat.
d	Thickness of coil insulation.
F	Total force of resistive hammer.
F_o	Total force on prefectly conducting hammer.
F_x	Force between mutually coupled coils axially spaced by 2x.
h	Thickness of hammer.
$i.$	Instantaneous current in driving circuit.
I_1	RMS current at which copper rivets melt.
I_2	RMS current at which aluminium rivets melt.
I_m	Maximum current in driving circuit.
k_x	Factor to account for effect of hammer resistance.
L_{11}	Self inductance of driving coil.
L_{12}	Mutual inductance between driving coil and its image.
L_S	Source inductance of driving circuit.
m	Mass of moving parts
P	Pressure due to magnetic field
r_c	Inner radius of coil
r_H	Outer radius of hammer.
R	Resistance of driving circuit
S	Sum of $d + \delta + x$
t	Time after closure of trigatron (Fig.2).
T	Temperature attained by conducting slab.
v	Velocity of rivet at time t.
V	Initial voltage on driving circuit capacitor, C.
W	Electrical energy input to driving circuit.
x	Hammer displacement at time t.
β	Ratio 2nd/1st positive current peaks in load circuit.
δ	Skin depth
δ_h	Skin depth in hammer
η	Efficiency of energy conversion
μ_o	Permeability of free space
ρ	Resistivity of hammer
σ	Specific density of hammer metal
τ	Time constant of driving circuit.
φ_1	Flux linking driving coil
ω	Angular velocity

1. INTRODUCTION

For thermonuclear experiments it is often necessary to transfer energy rapidly from capacitors to coils and to short circuit (clamp) the coils at maximum current[1]. The physical requirements for a satisfactory clamp switch are more difficult to realise than those for a making switch. However, a range of gas discharge switches has evolved for clamping duty[2,3,4,5,6]. Recently interest has revived in mechanical switches because of their low contact resistance. The elimination of the energy losses associated with the arc in a gas discharge switch can increase, substantially, the current decay time-constant of a clamped circuit.

Mechanical switches of the type normally associated with short-circuit testing of conventional rotating machinery and switchgear have been used for both making and clamping duties[7,8].

Typically these switches close in milli-seconds and they have fairly high inductances. Consequently, they are not generally useful for the fast-pulse (fundamental frequencies in the range 10-200 k H_z) circuits of interest in this field. Also, their closing times are too inconsistent for satisfactory parallel operation.

The mechanical switch to be described has a low inductance (about 20 nH) and closes in 50 μsec with shot to shot variations (jitter) of ±1 μsec[9,10,11].

In fast circuits where this closing time is too long the initial clamping can be undertaken by a suitable switch of, say, the solid dielectric type[5,6] with a fast mechanical switch closing in parallel soon afterwards. The duty on the primary switch is much reduced using this technique and, provided the mechanical switch operates fast enough, the energy lost in the arc is negligible. Both the speed and consistency of operation of the present switch appear quite adequate for duties of this type.

Hellegourc'h[12] has developed a switch similar to the present one but using larger rivets and designed for lower voltage circuits.

Marshall et al[13] have made a switch that closes in 15 μsec. In this switch busbar-like electrodes are distorted into contact by explosively fusing a metal ribbon in close proximity.

2. PRINCIPLES OF THE SWITCH

The basic components of the switch are illustrated in Fig.1 and the operating circuit is shown in Fig.2. The switch is closed by discharging the capacitor 'C' into the driving coil. The kinetic energy imparted to the hammer is dissipated driving the rivet through the polythene sheet and deforming the rivet against the anvil. The rivet, expendable electrodes and the polythene sheet are replaced after each closure.

2.1 The Dielectric

To make a fast mechanical switch it is obviously desirable to keep the travel of the moving contact as small as possible. By this means the closing time, jitter and driving energy are minimised. Using a fairly highly stressed solid dielectric between the electrodes the required travel can be kept very small indeed without compromising the reliability of the switch in terms of voltage withstand, but extra driving energy has to be supplied to penetrate the dielectric during the closing operation.

The minimum thickness of insulation depends upon the voltage of the circuit in which the switch is used, including any transient over-voltages (e.g. cable reflections) which can occur. We have used polyethylene sheet, 0·5 mm thick, in this switch. The choice of thickness to match particular voltage requirements is discussed briefly in Ref.5. Polyethylene is also suitable mechanically because it is soft and cuts easily.

Polyethylene, when subjected to both pressure and high electric stress, is an unreliable dielectric, probably because it extrudes fairly easily. The chosen electrode arrangement therefore clamps the polyethylene sheet only firmly enough to locate it.

2.2 The Rivetted Contact

The soft copper rivet absorbs the kinetic energy of the hammer so that there is no rebound with consequent damage to the driving coil. Coincidentally, the resulting deformation of the rivet improves the contact pressure in the hole and increases the contact area by splaying over the ends (see Fig.3.)

It has not been found necessary to provide any auxiliary guide for the rivet. It normally sits centrally on the hammer cap and is located in the lower electrode. By measuring the travel of the plunger and observing the time to make contact it has been found that the rivet has entered the hole in the upper electrode to a distance of 0·7 mm before contact is made. Thus the upper guide is established before the switch carries current and magnetic deflection of the rivet is not a problem. Sections taken through rivetted assemblies clearly indicate that polythene does extrude into the contact area and often right through the hole in the upper electrode in places. The extruded film appears to remain intact almost until the instant of metal-to-metal contact. This was shown by closing a 40 kV circuit in 58 μsecs which was only 7 μsec faster than closing a 30 volt circuit. The measured resistance (D.C.) of rivetted assemblies does not appear to vary according to whether the closure was made with or without current flowing through the switch, and in spite of the presence of extruded polythene, there is no evidence of carbon due to thermal degradation of polythene in the contact areas. Small variations in the clearance between the rivet and the holes in the electrodes do not noticeably affect the nature of the contact.

Comparative tests using aluminium (99·5% pure) and copper rivets have shown the superior current carrying capacity of copper. In pre-rivetted samples, using 12·7 mm diameter rivets, the aluminium rivets failed at 350 kA due to arcing in the joint whereas similar soft copper rivets survived 10 consecutive shots at 600 kA (600 coulombs). The contact failures appeared to stem from localised melting in the interface between the electrodes and the rivet. In section 9.1 we consider the conditions for surface melting using the assumption that the current skin depth is small compared with the radius of the rivet. This shows that the aluminium joint should be able to carry about 70% of the current carried by the copper joint. The tests show, however, that it will carry less than 60%. The implication is that better contact is achieved between copper and copper than between aluminium and copper.

3. THE ELECTROMAGNETIC DRIVE

The design of the drive is a very complex problem involving mutually interacting time and space variables. However, an attempt has been made, using a number of simplifying concepts to calculate the forces involved and the consequent motion of the rivet. Fig.4 shows that there is general agreement between the calculated and measured travel v. time characteristics of the rivet - good enough in fact to provide sufficient information for future designs.

The problem is simplified by assuming that the hammer is an infinite sheet and a perfect conductor. Then the hammer can be replaced by an image of the driving coil, using the base of the hammer as the plane of the symmetry. The force can be calculated now as the mutual interaction between similar coils carrying the same current (see section 9.2).

As the current initially flows on the inner surface of the coil all of the inductances can be calculated with sufficient accuracy by considering circular filamentary conductors of radius $(r_c + \delta/2)$ where r_c = inner radius of coil and δ = skin depth.

3.1 Energy Conversion and Current Wave Shape

With an input energy of 4 kJ the measured travel v. time characteristics of the drive show that the rivet in free flight reaches a constant velocity of 57 M/sec. The corresponding kinetic energy is 100 J for a 60 gm moving assembly; so that the energy conversion efficiency $\eta \simeq 2\%$. This measurement was made without clamp ignitrons (Fig.2) in circuit. Table 1 shows that this low efficiency is a direct consequence of using a damped oscillatory discharge.

The velocity of the hammer

$$v = \frac{1}{m} \int_0^t k\,(x)\,\frac{dL(x)}{dx}\; i^2\,dt \qquad \text{(Eqn.3, Section 9.2)}$$

(Zero initial conditions)

and typically, for this design,

$$v \simeq \frac{2\cdot 10^{-5}}{m} \int_0^t i^2\,dt$$

Whence the kinetic energy (= $\frac{1}{2}mv^2$) for various current wave forms can be compared using relative values shown in Table 1.

For $I_m = 10^5$A and $\omega = 10^5$ rad/sec,

and a square wave of current we obtain

$$W = 1.14.10^3 J$$

and $\eta \simeq 30\%$

These rough figures suggest that the maximum $\eta \simeq 30\%$ and that this can be bettered only by increasing the rate of change of mutual inductance between the drive coil and its image.

3.2 The Hammer

The position of the image coil, and consequently its coupling with the drive coil, is determined by the depth of current penetration into the hammer surface.

A high strength aluminium alloy * has been used for the hammer because, although it has about four times the specific resistivity ρ of copper, it is only one third as dense. As the penetration depth is proportional to $\rho^{\frac{1}{2}}$ there is only a small reduction in driving force due to decoupling. Experience has shown that this alloy is also strong enough to cope with the rather brutal treatment the hammer receives in the drive without distorting and binding in its guide.

A large diameter hammer is a good approximation to an infinite plane for the purposes of the idealised concept of section 3. The magnetic pressure however, decreases with radius so that for maximum acceleration there is an optimum size for the hammer. See section 9.3.

3.3 The Drive Coil

Details of the coil developed for use with this switch are shown in Fig.5. The helical arrangement allows for the turn adjacent to the hammer to be earthed. In practice the coil is clamped very tightly between substantial slotted stainless-steel plates so that the strain energy stored in the winding at maximum current does not tear the coil apart when it is released.

Coils have been tested on an 80 μF, 10 kV capacitor for more than 2000 operations without failure. The temperature rise is about 16°C with shots at 2 minute intervals on continuous runs.

4. CONSTRUCTION

The assembly of the switch is shown in Fig.6.

Using available capacitors, switches, etc. and simple layouts it is difficult to reduce the source inductance below 0·1 μH. Consequently the coil inductance must be of the order 1 μH so as to have most of the magnetic energy available at the drive. We have not been able to make reliable coils for working above 10 kV and this sets most of the working parameters as follows:-

The initial rate of rise of current $= \frac{V}{L} = 10^{10}$ A/sec.

The trigatron switch limits maximum current to about 100 kA - whence for a sinusoidal wave form

$$\omega I_m = 10^{10} \text{ A/Sec}$$

and $\omega = 10^5$ rad/sec (Frequency 16 KH_z)

and $c = 100$ μF and $W = \frac{1}{2} cv^2 = 5$ kJ

In the event we have used c = 80 μF and W = 4 kJ.

The expendable electrodes are accurately made from hard drawn copper strip and jig drilled in pairs. The rivet is made from annealed copper rod 12·7 mm dia. The holes in the electrodes are normally drilled 0·12 - 0·25 mm clearance on the rivet diameter, and the electrodes are aligned in the switch by means of dowels so that the holes are coaxial within ± 0·03 mm. The clearances quoted represent the extremes of the working ranges.

---

* HE 15 WP (Hiduminium 66) - Aℓ, 4% cu - B.S. 1476. Tensile strength 50 $Kg(mm)^{-2}$ or 32 tons $(inch)^{-2}$ in its heat treated and precipitated form.

If the rivet is too tight there is some drag and pick up of metal so that the switch operates slowly. If it is too loose the rivet is poorly formed and occasionally too much polythene is extruded into the joint with disastrous results because of arcing in the contact area.

The anvil is insulated from the upper electrode to prevent excessive buring (where its tip meets the rivet) prior to contact formation.

The spaces around the anvil and hammer are carefully ventilated to avoid air cushions which could retard the hammer.

5. SWITCH TESTS

5.1 Tests in a 40 kV circuit

The switch was tested in parallel with a fast solid dielectric switch[5] as shown in Fig.7. This arrangement is essentially that described in the introduction where the mechanical switch takes over from the arcing switch by reason of its low contact resistance. Fig.8 shows an oscillogram of a typical 100 kA test.

Using the 0·5 μH load coil for tests above 300 kA, the mechanical switch was used alone because of limitations in the arcing switch. The current rise time is 13 μsec in this circuit so that the switch was closed on the second positive current peak, i.e. about 65 μsec from closing the start switch. It was found that matching the closing time to the current wave form could be achieved either by delaying the triggering of the mechanical switch or more simply by adjusting the voltage on the driving circuit capacitor. Fig.9 is a series of oscillograms from these tests showing the characteristics of the switch closed onto a current peak in excess of 500 kA.

The voltage appearing across the switch (Fig.9c) in the 100 μsec or so after the closure is due to the switch inductance and is not a measure of contact resistance. At this current there are slight signs of arcing in the expended assemblies but not enough to impair the contact.

Fig.9d shows Fig.9c on an extended time scale to show that the contact is firmly established and maintained.

The charge passed by the switch is calculated from the equation

$$Q = \beta \frac{V}{R} (LC)^{\frac{1}{2}}$$

where β = ratio 2nd/1st positive current peak.
For $L = 0{\cdot}5\ \mu H$, $R = 185\ \mu\Omega$: $V = 40$ kV and $\beta = 0{\cdot}73$

$$Q = 1100 \text{ coulombs}$$

At this duty, viz 500 kA (peak), 1100 coulombs, 40 kV, (the maximum output of the test equipment), the switch was operated successfully for 50 consecutive closures.

5.2 Tests in a low voltage circuit

The switch was tested in the circuit shown in Fig.10 to establish the maximum current carrying capacity of 12·7 mm dia copper rivets.

The current rise time of this circuit is 470 μsec. The operation of the switch was delayed so as to close at the peak of the load current.

Fig.11 is an oscillogram in this series showing a successful closure at 600 kA (peak) with the switch passing about 2500 coulombs.

Fig.12 is an oscillogram showing a switch failure during 635 kA (peak) shot, where the arcing occurred just after the current peak. This repeats the experience on pre-rivetted assemblies mentioned in 2.2 and confirms estimated limits imposed by joule heating and magnetic pressure.

6. CONCULSIONS

This relatively unsophisticated switch is a useful addition to the range of fast, heavy duty switches now available in laboratories throughout the world. It fills a well known gap in the range, viz, the need for a switch with low contact resistance and an operating time less than 100 μsec.

The switch has been tested at full duty for 40 kV, 500 kA and a total charge of 1100 coulombs. The contacts have been tested up to 600 kA and a total charge of 2500 coulombs.

Used as a back-up switch the duty on primary arcing switches can be reduced considerably with consequent saving in contact erosion and maintenance. For example - if a 500 kA arcing switch is backed up by a rivet switch closing in 50 μsecs, the maximum charge passed by the arc is 25 coulombs.

The D.C. resistance of a rivetted contact (12•7 mm dia rivet) is 1-2 μΩ which compares with the usual few milli-ohms representing the arc drop in an arcing switch. Using this switch it is possible to increase the current decay time-constant of a clamped circuit without the need for expensive auxiliaries such as additional banks of low voltage capacitors.

7. ACKNOWLEDGEMENTS

The authors gratefully acknowledge the contributions of their colleagues. In particular we would like to thank Dr. L.L. Alston (now with the British Railways Board) who initiated this work, Mr. G.C. Barnes (now with the Australian Patents Office) and Mr. F.J.Hoare who contributed so much to the detailed design. To Mr. G.E. Austin we owe special thanks for his conscientious and unstinted experimental work. Mr. E.K. Sinton and Mr. M. Herring solved our mathematical problems using both the analogue and digital computers.
Mr. D. Griffiths (Northampton Polytechnic) and Mr. B.M. Ross (University of Aston) as vacation students contributed especially to detail development of the drive.

8. REFERENCES

1. SMART, D.L.: 'Some Switching problems in Thermonuclear Research', Proc. I.E.E., 1959, 106A, Suppl. 2, p.107.

2. HANCOX, R.: 'Low pressure gas discharge switches for use in fusion experiments', ibid 1964, 111, (1), p.203.

3. FITCH, R.A. and McCORMICK, N.R.: 'Low-inductance switching using parallel spark gaps', ibid., 1959, 106A, Suppl.2, p.117.

4. BISHOP, A.E. and EDMONDS, D.C.: 'Low-inductance 100 kV switch (Spark Gap) for starting, diverting and clamping capacitor discharges', ibid. 1966, 113 (9), p. 1549.

5. ALSTON, L.L., WHITTLE, H.R., MOSSON, G.A.G., and BARNES, G.C., 'Some experiments on a higher power closing switch with polythene as the main dielectric', ibid 1965, 112 (7), p.1424.

6. JAMES, T.E., HARRIES, K. and MEDFORD, R.D.: 'Development of fast 100 kV, 1 MA, solid dielectric switches and associated triggering systems', Proc. 1965 Symposium on Engineering Problems of Controlled Thermonuclear Research, Lawrence Radiation Laboratory, Livermore, CONF-650512.

7. BUTT, E.P., CARRUTHERS, R., MITCHELL, J.T.D., PEASE, R.S., THONEMANN, P.C., BIRD, M. A., BLEARS, J. and HARTILL, E.R. : 'The design and performance of ZETA'. Proc. I.E.E. 1959, 106A, Suppl. 2, p.12.

8. VIGREUX, J. : 'Court circuiteur ultra-rapide pour tres fortes intensities', Paper presented at 1962 Symposium on Engineering Problems in Thermonuclear Research, C.E.A., Fontenay-aux-Roses, Paris.

9. ROGERS, P.J.: 'A fast mechanical switch', paper presented at 1964 Symposium on Engineering Problems in Thermonuclear Research, Garching, Munich: Limited publication of proceedings.

10. WHITTLE, H.R.: 'Rivetted switch', British Patent Application No. C.40086/65.

11. ROGERS, P.J. and WHITTLE, H.R.: 'A fast mechanically closed switch', paper presented at 1966 Symposium on Engineering Problems in Thermonuclear Research, Frascati, Rome - Proceedings not published.

12. HELLEGOURC'H, J.: 'A fast mechanical switch', paper presented at 1966 Symposium on Engineering Problems in Thermonuclear Research, Frascati, Rome - proceedings not published.

13. MARSHALL, J., Los Alamos Scientific Laboratory of the University of California - Private communication.

14. HILL, M and MONTAGUE, R.G., 'Fast opening, all metal Gas Valves'. Culham Laboratory Memorandum (CLM-M62), 1966.

9. APPENDIX

9.1 Thermal rating of rivets

If the current penetration depth $\delta << r$ (the radius of the rivet) then the surface temperature of the rivet material is independent of specific resistivity of the rivet material.

Considering a slab model and a sinusoidal current waveform -

$$\int_0^t (I_m \sin \omega t)^2 \frac{\rho \ell}{\delta b} \, dt = \int_0^T \ell b \delta C_v \, dT$$

Where ℓ , b are surface dimensions
C_v = volumetric specific heat
T = temperature

for ½ cycle excitation - and considering Cv constant *

$$I_m^2 \frac{\pi}{2\omega} \frac{\rho \ell}{\delta b} = \ell b \delta \, C_v \, \Delta T$$

i.e.

$$\Delta T = \frac{I_m^2 \pi \rho}{2\omega \, b^2 \delta^2 C_v}$$

and substituting

$$\delta^2 = \frac{\rho}{\mu_o \omega}$$

$$\Delta T = \frac{I_m^2}{b^2} \frac{\pi \mu_o}{2C_v}.$$

Now if ΔT is defined as the temperature rise from ambient to the material melting point then geometrically similar rivets can be compared for current carrying capacities -

$$\frac{T_1}{I_2} = \left(\frac{I_1}{I_2}\right)^2 \left(\frac{C_{v_2}}{C_{v_1}}\right)$$

i.e.

$$\frac{I_1}{I_2} = (AB)^{½}$$

where A = ratio of melting point temperatures
B = ratio of volumetric specific heats

Now comparing aluminium and copper, $A \simeq 1{\cdot}65$ and $B \simeq 1{\cdot}28$ and

$$I_{cu}/I_{A\ell} \simeq 1{\cdot}45$$

---

* A reasonable approximation since its value changes by less than 30% between room temperature and the melting points of both Cu and Al.

9.2 Equations of Motion

Representing the hammer by an image of the driving coil as discussed in para (3.0), the force between mutually coupled coils is given by

$$F_x = -i_1 i_2 \frac{dL_{12}}{dx}$$

where L is the mutual inductance between the coils.

Now

$$F_x = L_{11} i_1 + L_{12} i_2$$

where φ_1 is the flux linking coil 1.

But to satisfy the requirements of the image

$$i_2 = -i_1$$

whence $L = L_{11} - L_{12}$ where L is the effective terminal inductance

and

$$\frac{dL}{dx} = \frac{dL_{12}}{dx}$$

The values L_{11}, L_{12}, and consequently L, can be calculated using the assumptions of para (3.0) for various relative positions of the two coils.

Considering the voltages around the drive circuit

$$\frac{1}{c}\int i dt + \frac{d}{dt}\left[\left\{L_s + L(x)\right\} i\right] + iR = 0$$

i.e.

$$\frac{1}{c}\int i dt + \left\{L_s + L(x)\right\} \frac{di}{dt} + i \frac{dL(x)}{dt} + iR = 0 \qquad \ldots(1)$$

where L_s is the source inductance.

The equation of motion is

$$m\frac{d^2x}{dt^2} = -i^2 \frac{dL_{12}(x)}{dx} = i^2 \frac{dL(x)}{dx} \qquad \ldots(3)$$

The two equations can be solved simultaneously using an analogue computer or step by step using a digital computer.

Now this argument relies upon the hammer being considered as a perfect conductor. This assumption, because it sets the image plane at the surface of the hammer, results in the coils of the model being more closely coupled than can be achieved in practice. Therefore it is necessary to adjust the calculated force by a factor which accounts for the fact that the flux density in the air gap between the coil and the hammer is lower than in the idealised case - some of the flux having been lost due to penetration into the hammer.

In our calculation of mutual inductances we have considered the distance between the coil and the image plane as

$$S = d + \delta + x$$

where x = distance of the hammer from its home position

d = thickness of insulation

δ = penetration depth in the coil

If the total flux in this gap is conserved, then allowing for penetration into the hammer the new flux density

$$B = \frac{B_o}{(1+\frac{\delta h}{S})}$$

where B_o is the idealised flux density

δ_h = penetration depth in hammer

and
$$F = \frac{F_o}{(1+\frac{\delta h}{S})^2}$$

where F_o is the idealised force.

Whence the equation of motion is modified to

$$m\frac{d^2x}{dt^2} = \frac{1}{(1+\frac{\delta h}{S})^2}\frac{dL(x)}{dx}i^2 = k(x)\frac{dL(x)}{dx}i^2 \qquad \ldots(3)$$

Fig.4 shows an analogue computer output using this equation - the measured curve is superimposed.

9.3 Hammer Dimensions

The field intensity in the air gap between the driving coil and the hammer can be approximated by assuming that all of the flux generated in the bore of the coil is constrained to pass through the air gap. Then if the field is considered as a two dimensional hydrostatic fluid exerting a pressure

$$p = B^2/8\pi \text{ dynes cm}^{-2} \qquad \text{(B in Gauss)}$$

the force exerted on the hammer is given by

$$F = \int_0^{r_c} \frac{B_c^2 r^3}{16S^2}dr + \int_{r_c}^{r_H} \frac{B_c^2 r_c^4}{r16S^2}dr$$

$$= \frac{B_c^2 r_c^4}{16S^2}\left[\tfrac{1}{4} + \ln\frac{r_H}{r_c}\right]$$

where B_c is the flux density on the centre line of the coil.

The mass of the hammer is given by

$$m = k_o + \pi r_H^2 h\sigma$$

where k_o is a constant representing the 'pay load' which includes the weight of the rivet and any other material which does not change as r_H is altered, and h is the thickness of the hammer considered as a disc of specific density σ. The thickness is set by mechanical strength and guidance requirements.

Then the initial acceleration is given by

$$\frac{F}{m} = \frac{k_2(\ln r_H - k_3)}{k_o + k_1 r_H^2}$$

where $k_1 = \pi h \sigma$

$$k_2 = \frac{B_o^2 \, r_c^4}{16S^2}$$

$$k_3 = \text{Ln } r_c - \tfrac{1}{4}$$

which, differentiated with respect to r_H and set equal to zero, yields

$$\text{Ln } r_H = 0{\cdot}5 + k_3 + \frac{k_o}{2k_1 r_H^2}$$

which is independent of B_o and S and is the condition for maximum acceleration of the hammer. For k_o = 20 gm, k_1 = 11 and K_3 = −0·22, the optimum hammer diameter is 35 mm.

TABLE 1

COMPARISON OF IMPULSES TO HAMMER FOR
VARIOUS CURRENT WAVEFORMS

current waveform	$\int_{t=0}^{t=2\pi/\omega} i^2 \, dt$	comparison of impulse values
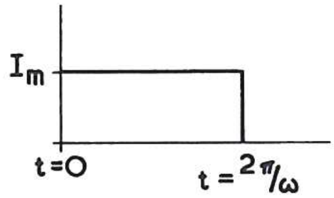 square wave	$2I_m^2 \, \pi/\omega$	1·0
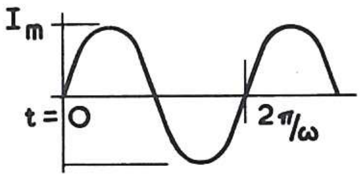 sine wave	$I_m^2 \, \pi/\omega$	0·5
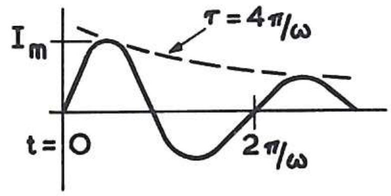 damped sine wave	$0{\cdot}64 \, I_m^2 \, \pi/\omega$	0·32
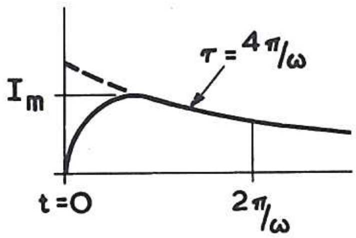 clamped circuit	$1{\cdot}35 \, I_m^2 \, \pi/\omega$	0·68

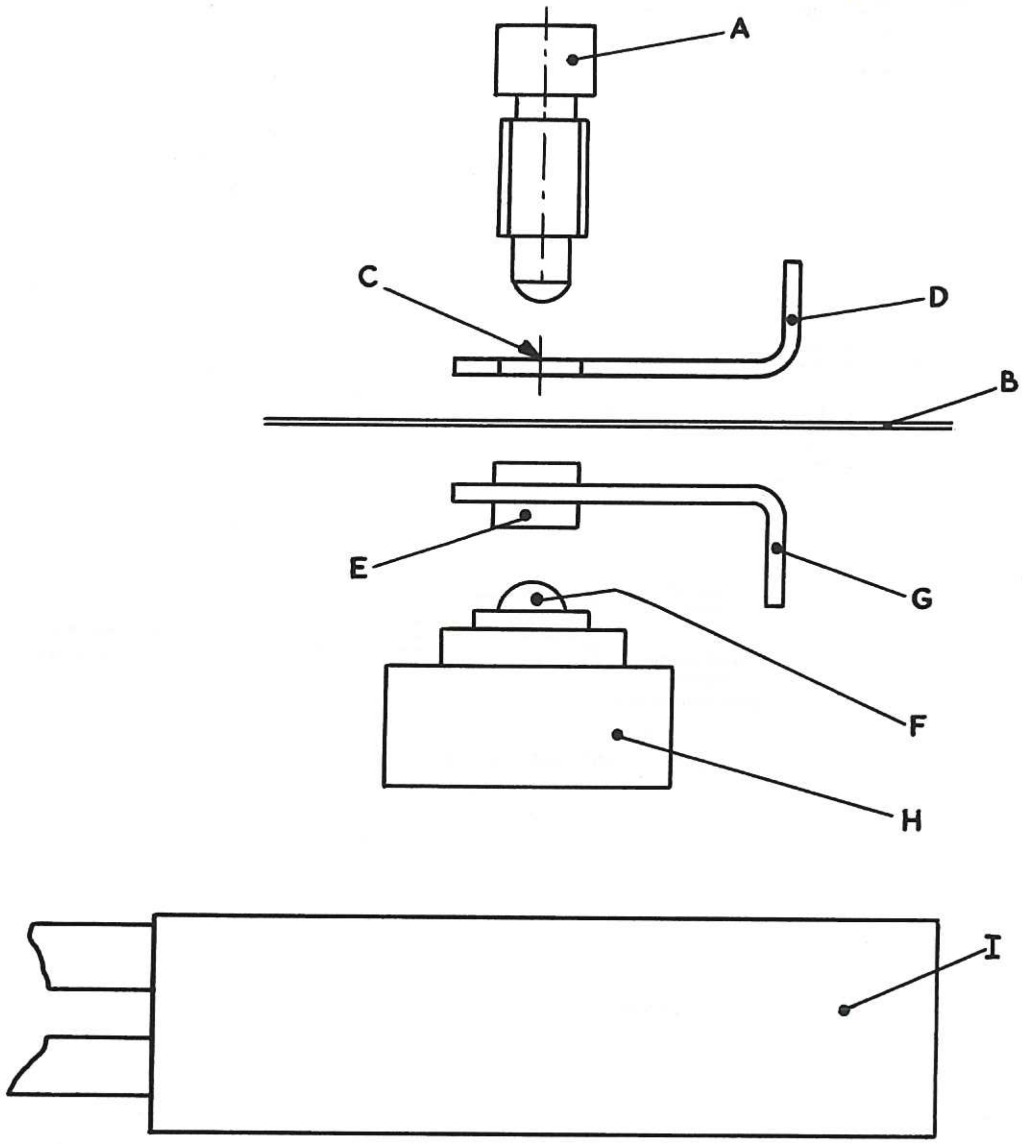

Fig. 1 Basic switch components (CLM-P 180)

A. Steel anvil
B. Polythene dielectric (0.5 mm thick)
C. Hole (12.8 mm dia).
D. Upper expendable copper L-piece (3 mm thick)
E. Soft copper cylinder 12.7 mm dia (Rivet)
F. Steel cap
G. Lower expendable copper L-piece (3 mm thick)
H. Dural hammer body (38 mm dia)
I. Driving coil (Cu/Be alloy, glass cloth insulation)

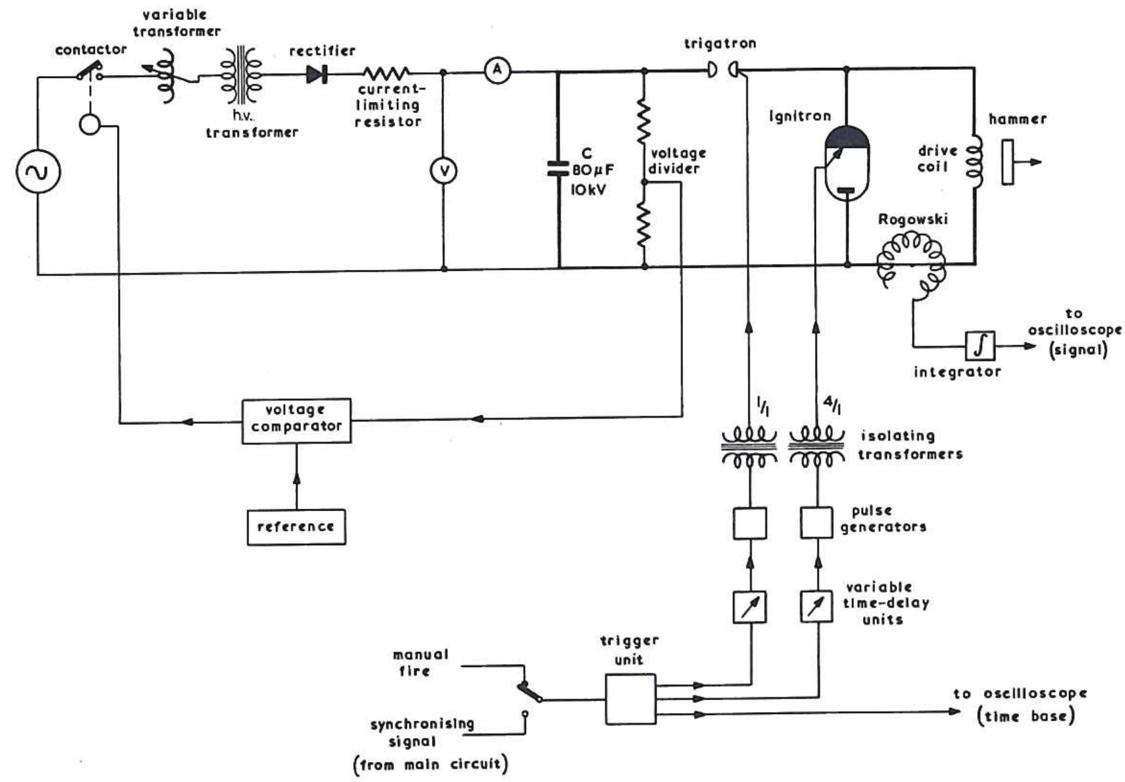

Fig. 2 Driving circuit (CLM-P 180)

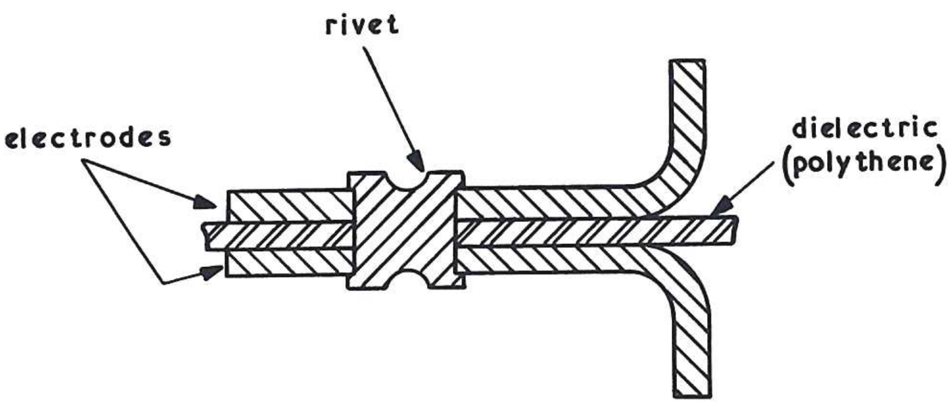

Fig. 3 Rivetted contact (CLM-P 180)

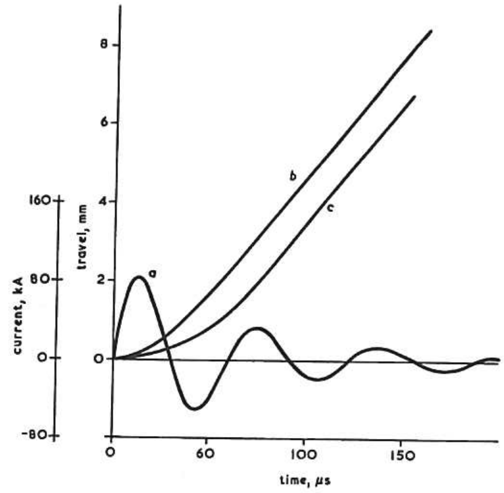

Fig.4 Hammer/rivet travel characteristics (CLM-P 180)
A = Calculated driving coil current
B = Calculated rivet travel
C = Measured rivet travel

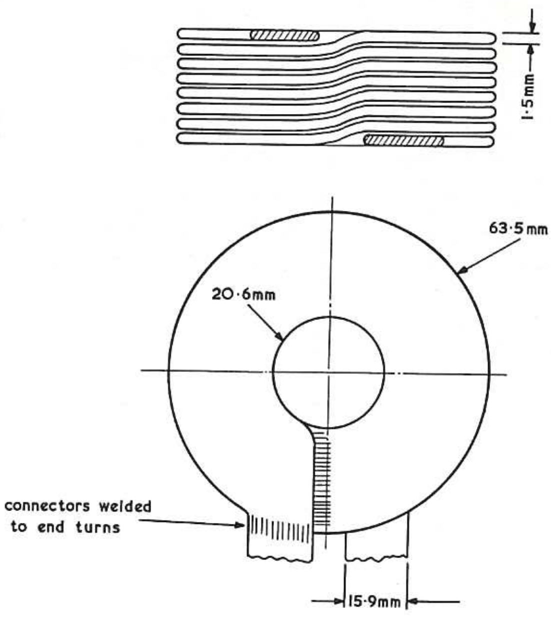

Fig.5 (CLM-P 180)
Driving coil details. Number of turns, 10; Material Cu/1.7% Be.

Manufacturing instructions

1. Machine from billet in half hard condition.
2. Anneal, 800°C for 20 mins. and water quench.
3. Bed turns in hydraulic press, 1600 kG.
4. Precipitation harden, 330°C for 45 mins, cool naturally in oxygen or wet hydrogen.
5. Insulate with 3 layers of 0.127 mm glass cloth.
6. Impregnate in plasticised epoxy resin.

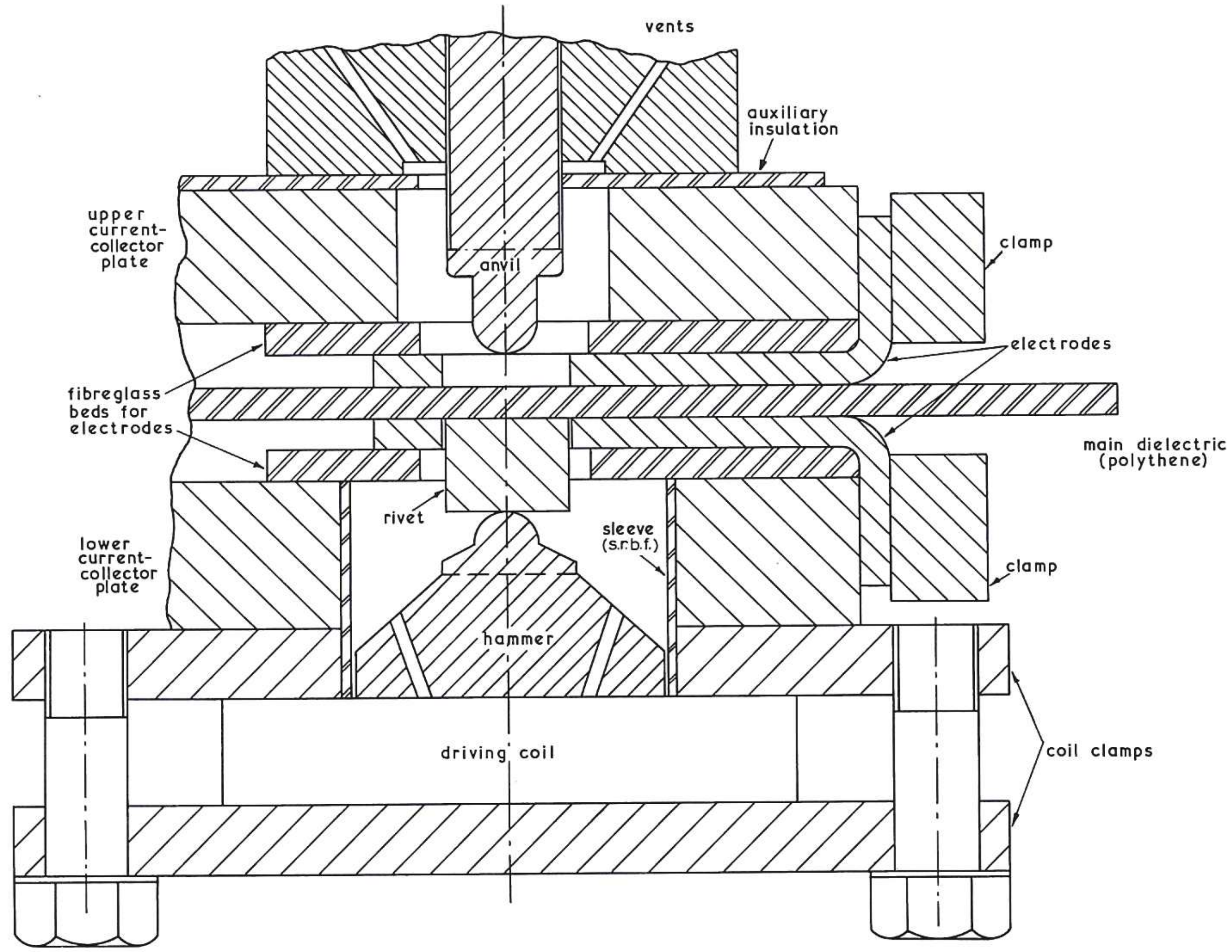

Fig. 6 Active elements of switch (CLM-P 180)

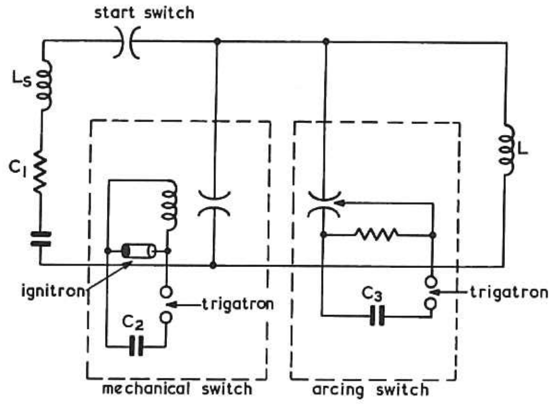

Fig.7 40 kV Test circuit (CLM-P 180)
C_1 = 96 μF, 40 kV (Main bank)
C_2 = 80 μF, 10 kV
C_3 = 1 μF, 20 kV
L = 10 μH or 0.5 μH (load inductance)
L_s = 0.24 μH (Source inductance)

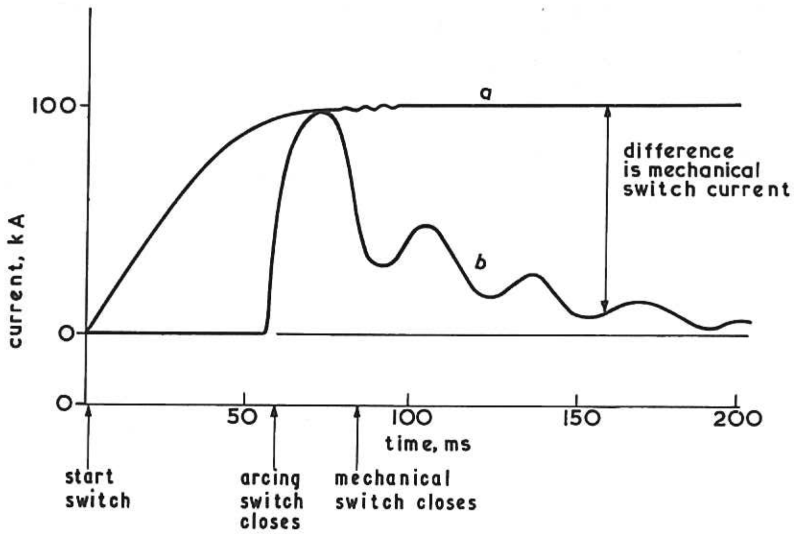

Fig.8 Waveshapes for 40 kV tests using 10 μH load coil (CLM-P 180)
A = Load current
B = Mechanical switch current
A-B = Mechanical switch current

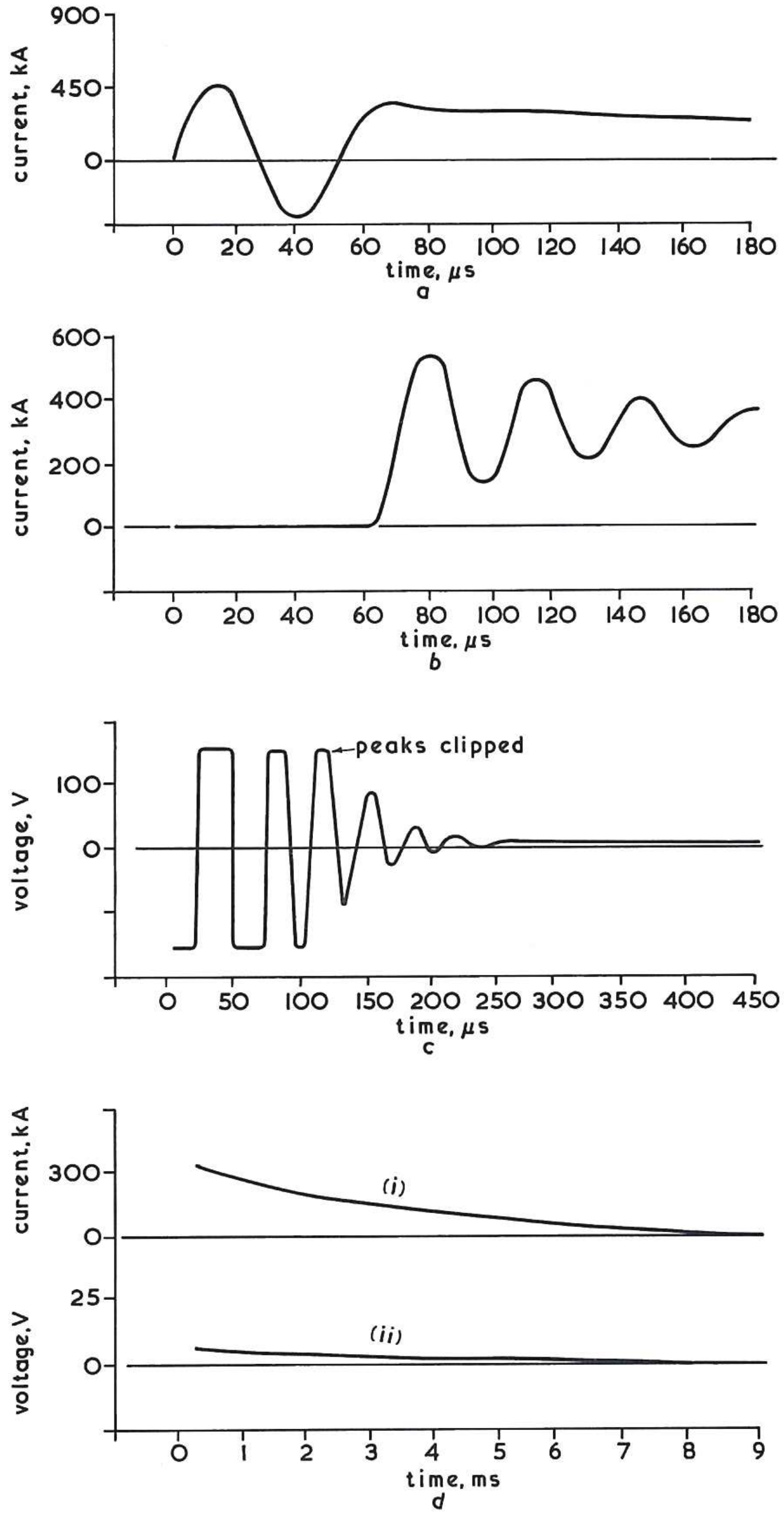

Fig. 9 Waveshapes for 40 kV tests using $0.5\,\mu$H load coil (CLM-P 180)
A = Load current
B = Mechanical switch current
C = Voltage across mechanical switch
D(a) = Mechanical switch current (longer time scale than (B))
(b) = Voltage across mechanical switch (longer time scale than (C))

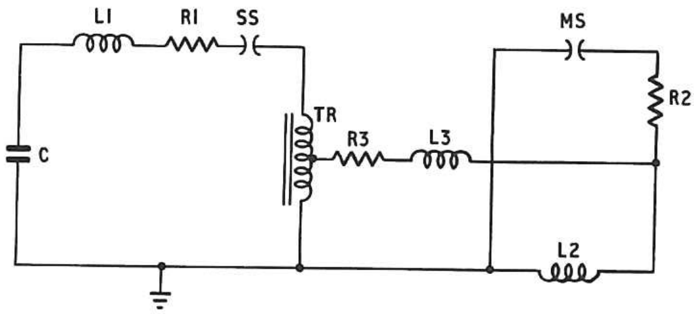

Fig. 10 Low voltage test circuit (CLM - P 180)

$C = 5150\,\mu F$, 20 kV (max)
L_1 = Source inductance ($5\,\mu H$)
L_2 = Load coil inductance (145 nH)
L_3 = Transmission line inductance (20 nH)
R_1 = Source resistance ($35\,m\Omega$)
R_2 = Clamped circuit resistance ($45\,\mu\Omega$)
R_3 = Transmission line resistance ($645\,\mu\Omega$)
T_R = Pulse transformer, coax cable type, ratio 15/1
SS = Start switch
MS = Mechanical switch

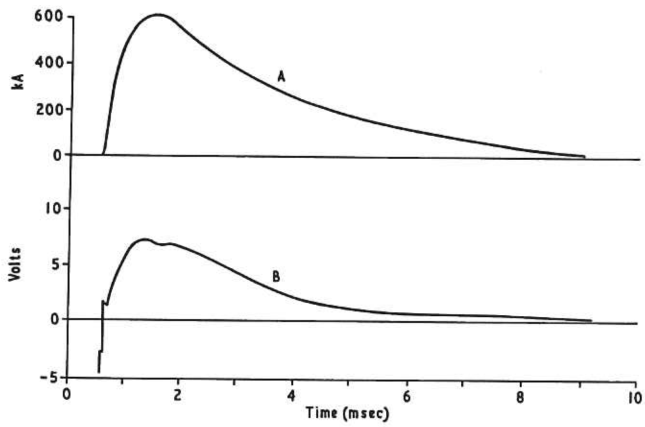

Fig. 11 Waveshapes for low voltage tests (CLM - P 180)
A = Mechanical switch current
B = Voltage across mechanical switch

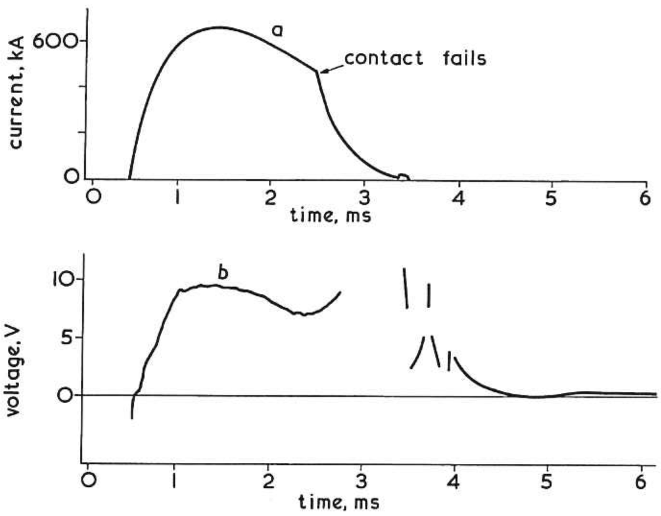

Fig. 12 Oscillogram of contact failure (CLM - P 180)
A = Mechanical switch current
B = Voltage across mechanical switch